Available online at www.sciencedirect.com
SCIENCE DIRECT®

Journal of the European Ceramic Society 24 (2004) 2509–2513

www.elsevier.com/locate/jeurceramsoc

A novel interfacial microstructure in $SrTiO_3$ ceramics with Bi_2O_3-doping

Ping-an Fang[a], Hui Gu[a,*], Hui Shen[a], Yuan-wei Song[a], Ping-chu Wang[a], Miran Čeh[b]

[a]*State Key Lab of High Performance Ceramics and Superfine Microstructures, Shanghai Institute of Sciences, Shanghai 200050, China*
[b]*Jožef Stefan Institute, Department of Nanostructured Materials, Jamova 39, Ljubljana, Slovenia*

Received 10 January 2003; received in revised form 31 May 2003; accepted 1 June 2003

Abstract

A novel interfacial microstructure was found in Bi_2O_3-doped $SrTiO_3$ ceramics. Bi-rich precipitates of sizes between 10 and 100 nm were observed at most grain boundaries. Using spatially-resolved EDS analysis, it was shown that these nano-precipitates had similar composition to $Sr_2Bi_4Ti_5O_{18}$ secondary phase formed at triple grain pockets. This was revealed by the same trends in both Bi/Ti and Sr/Ti ratios as a function of particle size. In addition to forming precipitates, Bi segregation was also detected at these boundaries. However, the segregation level was substantially lower compared with that at boundaries without precipitates. The latter type of boundaries was always covered with thin amorphous films. Such novel interfacial structure containing nano-particles at grain boundaries does not hinder the dielectric properties of the material and it cannot be simply incorporated into the grain–boundary–barrier–layer–capacitor (GBBLC) model, which requires continuous insulating layers.

Keywords: Amorphous films; Grain boundary; Interfaces; Nano-precipitate; Segregation; $SrTiO_3$

1. Introduction

One of the most important applications of $SrTiO_3$ polycrystalline ceramics is to use it as high-permittivity capacitors. Oxide dopants can promote the dielectric properties by forming insulating layers at grain boundaries,[1–3] which completely separate the semi-conductive $SrTiO_3$ grains, as explained using the grain–boundary–barrier–layer–capacitor (GBBLC) model proposed by R. Wernicke.[4] These insulating layers usually consist of a second phase, which is formed by reaction of the dopants with the matrix material.

The GBBLC model has been widely accepted and also applied to other dielectric systems such as Bi_2O_3-doped ZnO varistor materials.[5–9] In early 1980s, Franken et al.[10] observed 10–100 nm thick barrier layer together with adjacent 50–500 nm thick diffusion layers containing bismuth in Bi_2O_3-doped $SrTiO_3$ capacitor material. In contrast, Olsson et al.[11,12] found only 1–10 nm thick barrier layers in ZnO with no diffusion layer. Recently Wang[13] and co-workers reported on approximately 1 nm thick amorphous film at grain boundaries in Bi_2O_3-doped ZnO. It is also believed that the barrier layer in $SrTiO_3$ capacitor materials is formed by a nanometer thick amorphous film as observed in a Fe-doped sample.[14]

In this paper we present a study of microstructure in Bi_2O_3-doped $SrTiO_3$ ceramics, which was fired at relatively low temperature. A novel grain boundary structure was observed, which may help in better understanding of GBBLC model.

2. Experimental

A mixture of analytical-grade TiO_2 and $SrCO_3$ powders (Qingpu Corporation of Chemical Reagent, Shanghai) was calcined at 1100 °C for 1 h. The resulting $SrTiO_3$ powder was mixed with 1 mol% of Bi_2O_3–$3TiO_2$ and 0.3 mol% of Nb_2O_3 and 10 mol% of LiF as a sintering aid. After wet milling and drying, the powders were pressed into 2-mm thick pellets of 10 mm in diameter. The pellets were sintered at 1190 °C for 2 h in flowing N_2 gas with 10% H_2. The material was air cooled to room temperature in air at an average rate of 6 °C per minute. The dielectric properties of the material were measured with

* Corresponding author. Fax.: +86-21-52413122.
E-mail address: gu@mail.sic.ac.cn (H. Gu).

0955-2219/$ - see front matter © 2003 Elsevier Ltd. All rights reserved.
doi:10.1016/S0955-2219(03)00637-X

an impedance analyzer (Model HP4192, Hewlett-Packard, USA).

TEM specimens were prepared by mechanical grinding and polishing, followed by argon ion milling to reach electron transparency. TEM characterization was performed in a transmission electron microscope (Model JEM 2010, Jeol Co., Tokyo, Japan) operating at 200kV, which was equipped with an EDS system (Model Link-ISIS, Oxford Instrument, England) for chemical analysis. An effective electron probe of 35 nm in diameter was used for EDS investigation. Quantification of elemental ratios was based on the Cliff–Lorimer equation of EDS analysis. The *k*-factors there were calculated using the thin specimen routine and the ZAF corrections were also made.

3. Results and discussions

Thirty-five randomly selected grain boundaries (GB) were analyzed in the specimens. Nano-sized precipitates were found at two thirds of them. Typical boundaries containing precipitates are shown in Fig. 1a and b. The size of precipitates ranged from 10 to 100 nm. Other grain boundaries without such precipitates were always covered with inter-granular amorphous films of thickness about 1 nm, as revealed by HRTEM and/or Frensel contrast (Fig. 1c). Additionally, large particles were observed at triple pockets (TP), as shown in Fig. 1d. The size of these particles was in the range 100–700 nm.

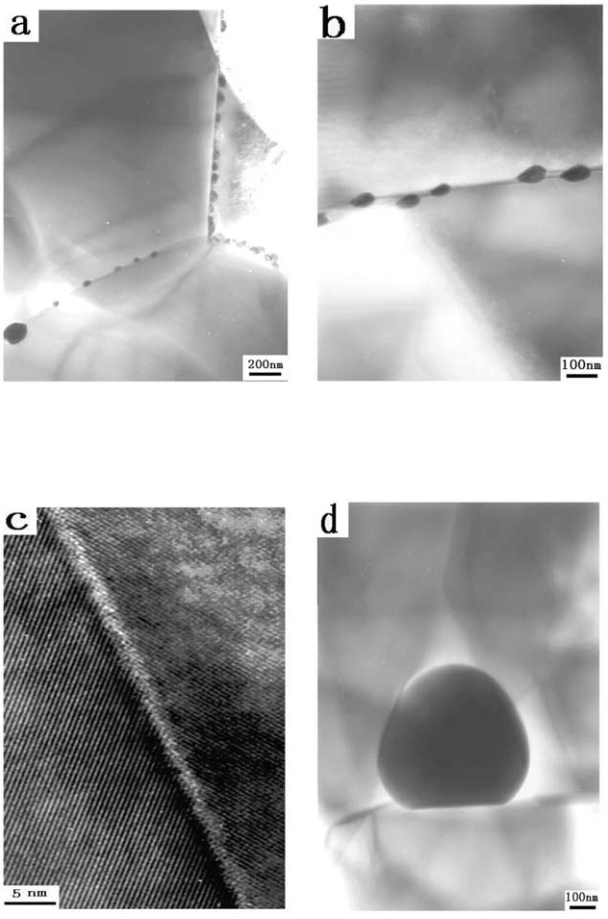

Fig. 1. Typical interfacial microstructures in a Bi_2O_3-doped $SrTiO_3$ material: grain boundaries with nano-precipitates (a, b), grain boundaries with thin amorphous film of thickness about 1 nm (c) and second-phase particles formed at triple-pockets (d).

The composition of nano-precipitates at grain boundaries could not be probed directly by EDS analysis. This is because most precipitates were smaller than or comparable with the broadened probe size; therefore, the spectra measured from precipitates contained contributions from the surrounding $SrTiO_3$ matrix. To evaluate this contribution, we plotted the Bi/Ti and Sr/Ti ratios measured on precipitates and particles against their size as showed in Fig. 2. Correlations between these parameters were revealed. Both Bi/Ti and Sr/Ti ratios follow linearly the precipitate size, indicating a rather uniform composition of precipitates. When the size of precipitate exceeded the effective probe size and the specimen thickness (at approx. 100 nm), both ratios reached their respective plateaus since there was no longer any contribution from $SrTiO_3$ grains. The measured Bi/Ti and Sr/Ti ratios of the precipitates at grain boundaries approached those of particles at triple pockets, indicating that the nano-precipitates possess the same composition. This unified plot suggests a common phase for the precipitates at grain boundaries and the particles in triple pockets.

An additional result on the overall composition of the sample was obtained by X-ray diffraction analysis (XRD) of the investigated material, which revealed a small amount of the secondary phase $Sr_2Bi_4Ti_5O_{18}$ besides the $SrTiO_3$ matrix. Quantification of the EDS spectra of the particles at the triple points gave Sr:Bi:Ti ratio to be 2.1:4.3:5.2, which agrees well with the corresponding atomic ratio for the $Sr_2Bi_4Ti_5O_{18}$ compound, i.e. the secondary phase. According to Fig. 2, the nano-precipitates and the large particles are the same phase. Therefore, the novel interfacial structure thus consists of $Sr_2Bi_4Ti_5O_{18}$ nano-precipitates at the grain boundaries in $SrTiO_3$.

In order to understand the mechanism of second phase precipitation at the grain boundaries and why some other boundaries do not exhibit such precipitation, we compared the segregation behavior for two different types of grain boundaries. EDS profile analyses were performed for boundaries with and without precipitates, as shown from Bi/Ti profiles in Fig. 3. For the boundary with precipitates, the probe was scanned across a boundary segment between the precipitates. The Bi/Ti profile revealed that Bi concentration at the grain boundaries without precipitates was significantly larger as compared to those containing the nano-precipitates. The precipitation-free boundaries were usually

covered with continuous amorphous layers (Fig. 1c), which should be composed of segregated Bi as has been reported elsewhere.[13] The boundaries with precipitates were depleted of such films and exhibited much less Bi segregation.

The de-segregation or de-wetting effect of Bi and the formation of nano-precipitates at some grain boundaries indicates that the precipitates were formed as a consequence of attaining the equilibrium grain boundary configuration. The additive LiF as sintering aid, whose melting point is 845 °C, can effectively promote the liquid phase sintering. It should be noted that LiF has relatively high volatility at the sintering temperature and can easily evaporate during sintering. Indeed, no fluorine signal was detected in this sample with EDS. Therefore, almost no LiF left in grain boundary films after sintering. During sintering all grain boundaries were permeated liquid phase, as schematically shown in Fig. 4a, since the melting point of Bi_2O_3 is only 825 °C and the Bi_2O_3–TiO_2 eutectic temperature is about 750 °C. Upon cooling, wetting film remained at some boundaries, while the de-wetting and precipitation was

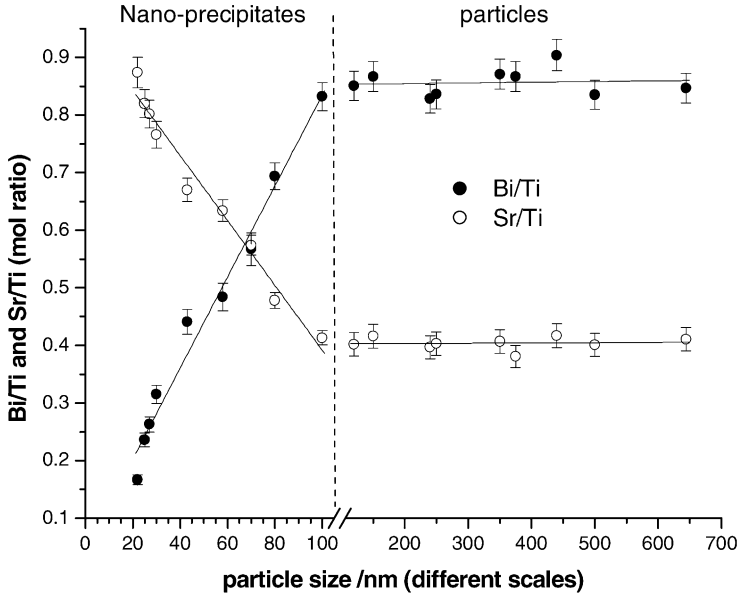

Fig. 2. Bi/Ti and Sr/Ti ratios versus the sizes of nano-precipitates at grain boundaries and particles at triple pockets.

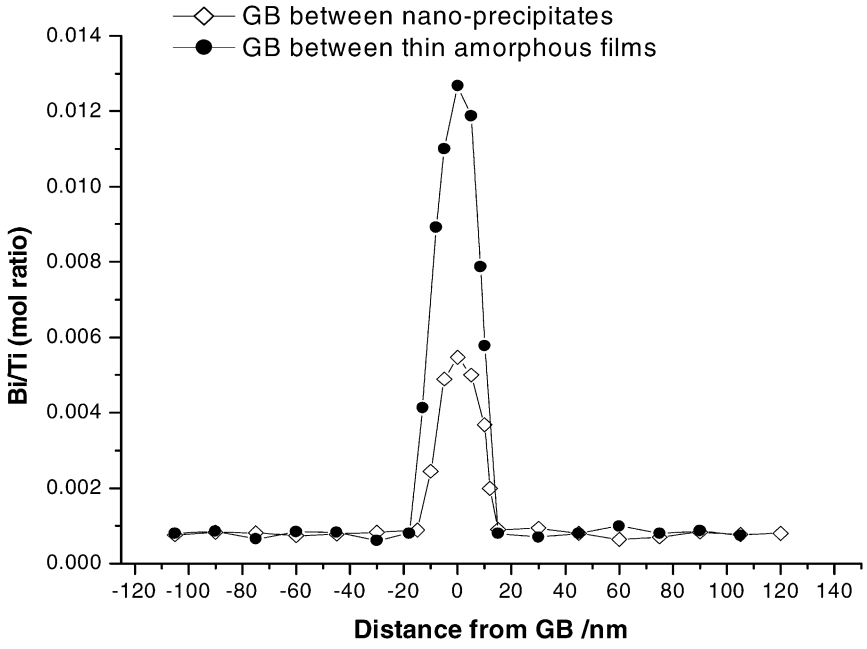

Fig. 3. Bi/Ti ratios across two types of grain boundaries to reveal different segregation behaviors.

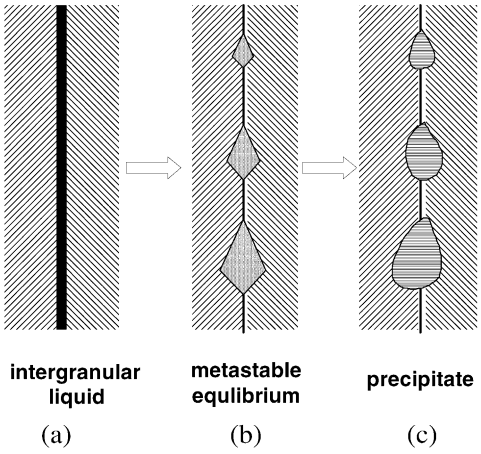

Fig. 4. Schematic description for formation of nano-precipitates at de-wetted grain boundaries (see details in text).

triggered on some other boundaries in order to lower grain boundary energy. It can be suggested that the process of precipitation occurred in two steps according to their specific shape. At first, nano-pockets of amorphous segregates were created at the grain boundary due to the combined effect of grain boundary de-wetting and a low diffusion rate, the latter limited the migration of segregants towards triple pockets (Fig. 4b). Second, the amorphous nano-pockets crystallized into $Sr_2Bi_4Ti_5O_{18}$ nano-particles (Fig. 4c). Similar facetted amorphous nano-pockets in a non-wetting grain boundary have been reported in other model systems, such as SiO_2 pockets in $\Sigma 33$ boundary in Si-bicrystal[15] and faceted pockets in $\Sigma 5$ boundary in $SrTiO_3$-bicrystal.[16] Further work is needed to establish the correlation between nano-precipitates and de-wetted boundaries.

The absence of a continuous barrier layer to separate the individual semi-conductive $SrTiO_3$ grains, as observed in our material, may not provide sufficient dielectric contribution in terms of GBBLC model. However, the examined material exhibited high permittivity. Its effective dielectric constant (ϵ) and loss factor ($\tan\delta$) were 3.2×10^5 and 4×10^{-2} at 1 kHz, respectively.[17] Although the e is an order lower than the latest reported results with significant Ba solution, it is still substantially higher than the other reported $SrTiO_3$-based ceramics.[10,18–20] It is unlikely that the amorphous films in only one third of the grain boundaries could alone contribute to the measured dielectric properties, without other boundaries being more or less insulating as well. It was therefore concluded that the majority of de-wetted boundaries containing precipitates undoubtedly able to play an important role in adding to the insulating nature of the boundary system, which is likely to be associated with the presence of regularly spaced precipitates.

Similarly, Olsson and Dunlop[12] have found that different types of interfaces, as well as inter-granular junctions, could act as barriers to electrical conduction and had influence on the current-voltage characteristics in Bi_2O_3-doped ZnO varistor materials. Franken et al.[10] believed that the contributions to the effective dielectric constant of Bi_2O_3-doped $SrTiO_3$ material came from both the amorphous boundary layer and the $Sr_2Bi_4Ti_5O_{18}$ second phase. The presently observed interfacial microstructure containing $Sr_2Bi_4Ti_5O_{18}$ nano-precipitates dispersed along grain boundaries could contribute to insulating barriers for dielectric performance, especially at high frequency. On the other hand, such boundaries would be less efficient as barriers compared to continuous amorphous films for low frequency. It is therefore reasonable to assume the synergetic effect of precipitates and amorphous film at the grain boundary will contribute to the relatively high dielectric property observed in this material.

4. Conclusions

A novel interfacial structure with nano-precipitates along grain boundaries was found in $SrTiO_3$ ceramics doped with 1.0 mol% Bi_2O_3. Quantification of EDS spectra revealed that nano-precipitates had similar composition as $Sr_2Bi_4Ti_5O_{18}$ secondary phase found at triple pockets. Other grain boundaries free of any precipitates were covered with amorphous films, which had significantly stronger Bi segregation compared with the grain boundaries containing the nano-precipitates. The concurrent de-segregation and de-wetting effects at grain boundaries with nano-precipitates indicates that they were formed as a part of equilibrium configuration for some grain boundaries. The high dielectric property of this sample results most probably from synergetic effect of the nano-precipitates and the amorphous film at the grain boundaries.

Acknowledgements

The authors acknowledge the financial supports by Chinese Natural Science Foundation (grant no. 50272074) and Shanghai Science and Technology Development Foundation (grant no. 0159nm075) as well as the travel supports by Ministries of Science and Technology of China and Slovenia.

References

1. Qi, J. Q., Chen, W. P., Wu, Y. J. and Li, L. T., Improvement of the PTCR effect in $Ba_{1-x}Sr_xTiO_3$ semiconducting ceramics by doping of Bi_2O_3 vapor during sintering. *J. Am. Ceram. Soc.*, 1998, **81**(2), 437–438.
2. Nishigaki, S., Murano, K. and Ohkoshi, A., Dielectric properties of ceramics in the system $(Sr_{0.5}Pb_{0.25}Ca_{0.25})TiO_3$–$Bi_20_3{\cdot}3TiO_2$ and

their applications in a high-voltage capacitor. *J. Am. Ceram. Soc*., 1982, **65**(11), 554–560.
3. Bongers, P. F. and Franken, P. E. C., Secondary phases and segregation layers at grain boundaries in electronic ceramic materials. In *Advances in Ceramics,* Vol. I, ed. L. M. Levinson. The American Ceramic Society, Columbos. Ohio, 1981, pp. 38–52.
4. Wernicke, R., Two-layer model explaining the properties of $SrTiO_3$ boundary layer capacitor. In *Advances in Ceramics,* Vol. I, ed. L. M. Levinson. The American Ceramic Society, Columbos. Ohio, 1981, pp. 272–281.
5. Clark, D. R., The microstructure location of the intergranular metal-oxide phase in a zinc oxide varistor. *J. Appl. Phys*., 1978, **49**(4), 2407–2411.
6. Wong, J. and Morris, W. G., Microstructure and phases in nonohmic ZnO–Bi_2O_3 ceramics. *Ceram. Bull*., 1974, **53**(11), 816–820.
7. Morris, W. G., Electrical properities of ZnO–Bi_2O_3 ceramics. *J. Am. Ceram. Soc*., 1982, **56**(7), 360–364.
8. Wong, J., Nature of intergranular phase in nonohmic ZnO ceramics containing 0.5 mol% Bi_2O_3. *J. Am. Ceram. Soc*., 1974, **57**(8), 357–359.
9. Gambino, J. P., Kingery, W. D., Pike, G. E., Levinson, L. M. and Philipp, H. R., Effect of heat treatments on the wetting behavior of bismuth-rich inter-granular phases in ZnO:Bi:Co varistors. *J. Am. Ceram. Soc*., 1989, **72**(4), 642–645.
10. Franken, P. E. C., Viegers, M. P. A. and Gehring, A. P., Microstructure of $SrTiO_3$ boundary-layer capacitor material. *J. Am. Ceram. Soc*., 1981, **64**(12), 687–690.
11. Olsson, E., Falk, L. K. L. and Dunlop, G. L., The microstructure of a ZnO varistor material. *J. Mater. Sci*., 1985, **20**, 4091–4098.
12. Olsson, E. and Dunlop, G. L., Characterization of individual interfacial barriers in a ZnO varistor material. *J. Appl. Phys*., 1989, **66**(8), 3666–3675.
13. Wang, H. F. and Chiang, Y. M., Thermodynamic stability of inter-granular amorphous films in bismuth-doped zinc oxide. *J. Am. Ceram. Soc*., 1999, **81**(1), 89–96.
14. Gu, H., Tendency and scale of chemistry and bonding changes at $SrTiO_3$ grain boundaries by Fe segregation. *Mat. Res. Soc. Symp. Proc*., 1997, **458**, 115–120.
15. Duscher, G., *Oxidische Korngrenzenphasen im Silicium.* PhD thesis, Stuttgart University 1996 (in German).
16. Dravid, V. P. and Ravikumar, V., Atomic structure and properties of the (310) symmetrical tilt grain boundary (STGB) in $SrTiO_3$. Part 2: Comparison with experimental studies. *Interface Science*, 2000, **8**(2/3), 177–187.
17. H., Shen, *Investigation on $SrTiO_3$-based Grain Boundary Barrier Layer Capacitor (GBBLC) Material Single-Fired under Low Temperature*. Master thesis, Shanghai Institute of Ceramics, 2001 (in Chinese).
18. Shen, H., Song, Y., Gu, H., Wang, P. and Xi, Y., A high-permittivity $SrTiO_3$-based grain boundary barrier layer capacitor material single-fired under low temperature. *Mater. Lett*., 2002, **56**, 802–805.
19. Laurent, M. J, Desgardin, G., Raveau, B., Haussonne, J. M. and Lostec, J., Sintering of strontium titanate in the presence of lithium salts in a reducing atmosphere. *J. Mater. Sci*., 1988, **23**, 4481–4486.
20. Zhou, L., Jiang, Z. and Zhang, S., Electrical properties of $Sr_{0.7}Ba_{0.3}TiO_3$ ceramics doped with Nb_2O_5, $3Li_2O$-$2SiO_2$ and Bi_2O_3. *J. Am. Ceram. Soc*., 1991, **74**(1), 2925–2927.